An extensive set of data for methoxide exchange, eq 10.3, has $\Delta S^{\ddagger} = -18$, and for $CH_3COOAr + CH_3O^-$, $\Delta S^{\ddagger} = -21$.[54] Entropies for ionic reactants in methanol are affected to an unknown extent by ion pairing, and in water presence of ions complicates the prediction of the entropy for hydroxide-catalyzed hydrolysis. It is certainly possible that one or more extra molecules of water are hydrogen bonded in the transition states.

Energy diagrams for reaction coordinate states can be constructed in part for hydroxide-catalyzed hydrolysis of esters. Figure 1 shows the known energy values for three esters.[71,72] For ethyl acetate $\Delta G^{\ddagger} = 16.3$ kcal mol^{-1} and ΔG(products - reactants) for hydrolysis to neutral products is -1.7 kcal mol^{-1}. The corresponding values for phenyl acetate are 14.9 and -7.4; for *p*-nitrophenyl acetate they are 13.6 and -9.4. For an ester ZCOOZ' such as $CF_3COOC_6H_3(NO_2)_2$ having strongly polar substituents, $\Delta G^{\ddagger}$ is predicted to be about 5.5 = 16.3 - (0.47(12) + 0.26(8)1.4 and $\Delta G = -20$ or less. The energies shown for the tetrahedral intermediates T and for the second transition state are speculative.

Acknowledgment. This work was supported by the National Science Foundation. I am deeply appreciative of critical and thoughtful comments provided by W. P. Jencks, J. F. Kirsch, and G. L. Schmir.

Registry No. 1, 495-78-3; **2**, 24423-04-9; **3**, 40662-08-6.

(70) Rate data reported[69] at 20 °C and at 50 °C yield the following Arrhenius activation energies for RCOOMe + NaOH in 40% aqueous dioxane; units are k_{cal}/mol: Me 10.9, Et 10.0, *n*-Pr 11.4, *n*-Bu 9.8, *i*-Bu 10.9, *i*-Pr 10.0, *s*-Bu 10.7, *t*-Bu 10.9. The data are anomalous in that most of the rate variations here are due to the *A* factor (the $\Delta S^{\ddagger}$ term) while in other studies[67-68] $\Delta S^{\ddagger}$ values are relatively constant for the series. The $\Delta S^{\ddagger} = -27$ for methyl acetate.

(71) Gerstein, J.; Jencks, W. P. *J. Am. Chem. Soc.* **1964**, *86*, 4655-4663.
(72) The $\Delta G^{\ddagger}$ values were computed from the rate constants.[55,56]

Cadmium Binding by Biological Ligands. 1. Formation of Protonated Polynuclear Complexes between Cadmium and D-Penicillamine in Aqueous Solution

Alex Avdeef* and Diane L. Kearney

Contribution from the Department of Chemistry, Syracuse University, Syracuse, New York 13210. *Received June 18, 1981*

Abstract: Extensive alkalimetric titrations of the cadmium-D-penicillamine system in aqueous solutions have revealed the presence of several protonated polynuclear metal complexes in the pH 4-8 region. Over 1000 pH measurements (glass electrode), in 15 separate titrations, were collected with a computer-controlled titrator. The solutions [25 °C, 0.2 M (KNO_3) ionic strength] contained 1-5 mM cadmium nitrate and a 3-fold (or more) excess of D-penicillamine. The functional behavior of the data was consistent with the equilibrium model employing the species $Cd(pen)H^+$, $Cd_3(pen)_4H_2$, the "core + link" series $Cd_2(pen)_5H_3[Cd(pen)H]_n^{n-3}$, $n = 0, 1, 2...$, $Cd(pen)_2^{2-}$, and $Cd(pen)_2OH^{3-}$.

The amino acid D-penicillamine, I, has attracted considerable

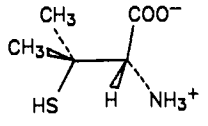

I

attention in heavy metal poisoning.[1,2] Although the molecule is effective in chelation therapy for copper, lead, and mercury poisoning, it appears to *elevate* the toxicity of cadmium, for reasons not entirely understood.[3]

The interpretation of the biological binding mechanisms of cadmium can be assisted by the understanding of the metal binding mechanisms in simple aqueous solutions containing a controlled and limited number of ligands. Unfortunately, the vast majority of older studies of cadmium reactions with sulfhydryl ligands are incomplete. Such reactions can be much more complicated than first realized, due to the propensity of sulfhydryl groups to bridge metal ions to form polynuclear complexes.[4] In aqueous solution the determination of the composition of such species is often a difficult endeavor, especially when several polynuclear species exist simultaneously with comparable concentrations.[5]

Past studies of the equilibrium complexation reactions of the cadmium-penicillamine system have not substantiated the presence of polynuclear complexes in low ionic strength ($\leq$0.2 M) aqueous solution for metal concentrations at the millimolar level. Kuchinkas and Rosen,[6] Lenz and Martell,[7] and Sugiura et al.[8] interpreted equilibrium data with the species Cd(pen) and $Cd(pen)_2$, where pen = penicillamine. Corrie et al.,[9] in the most comprehensive study to date, proposed a model consisting of several protonated mononuclear complexes. Apparently at the 3 M ionic strength used, polynuclear complexes are not observed to form. Sovago et al.[10] suggested that the methyl groups on penicillamine sterically hinder the formation of certain polynuclear complexes. In the solid state, however, penicillamine is known to coordinate cadmium in a polymeric fashion.[11,12] In contrast to the case of penicillamine, cysteine forms polynuclear species with cadmium in dilute solution, as first indicated by Perrin and Sayce.[13]

(1) Goodman, L. S.; Gilman, A., Eds. "Pharmacological Basis of Therapeutics", 5th ed.; Macmillan: New York; 1975; Chapter 11.
(2) Gergely, A.; Sovago, I. *Met. Ions Biol. Syst.* **1979**, *9*, 77-102.
(3) Lyle, W. H.; Green, J. N.; Gore, V.; Vidler, J. *Postgrad. Med. J.* **1968**, *44* (suppl), 18-21.
(4) DeBrabander, H. F.; VanPoucke, L. C. *J. Coord. Chem.* **1974**, *3*, 301-306.
(5) Sillén, L. G. In "Coordination Chemistry"; Martell, A. E., Ed.; Van Nostrand Reinhold: New York, 1971; A.C.S. Monogr. 168, Vol. 1, Chapter 9.
(6) Kuchinkas, E. J.; Rosen, Y. *Arch. Biochem. Biophys.* **1962**, *97*, 370-372.
(7) Lenz, G. R.; Martell, A. E. *Biochemistry* **1964**, *3*, 745-750.
(8) Sugiura, Y.; Yokoyama, A.; Tanaka, H. *Chem. Pharm. Bull.* **1970**, *18*, 693-701.
(9) Corrie, A. M.; Walker, M. D.; Williams, D. R. *J. Chem. Soc., Dalton Trans.* **1976**, 1012-1015.
(10) Sovago, I.; Gergely, A.; Harman, B.; Kiss, T. *J. Inorg. Nucl. Chem.* **1979**, *41*, 1629-1633.
(11) Freeman, H. C.; Hug, F.; Stevens, G. N. *J. Chem. Soc., Chem. Commun.* **1976**, 90-91.
(12) Carty, A. J.; Taylor, N. J. *Inorg. Chem.* **1977**, *16*, 177-181.

0002-7863/82/1504-7212$01.25/0

Table I. Equilibrium Data

set no.	total concn, mM $Cd(NO_3)_2$	D-pen	HNO_3	KNO_3	no. of pts
		Group I			
1	0	4.52	18.56	177.2	75
2	0	6.80	17.57	176.0	75
3	0	8.50	17.63	174.3	77
		Group II			
4	0.78	14.90	17.63	179.7	73
5	1.56	14.90	18.63	176.6	72
6	2.34	14.90	19.36	173.3	73
7	3.12	14.90	20.26	170.1	73
8	3.90	14.90	20.99	166.7	36
9	4.69	14.90	21.85	163.5	75
		Group III			
10	3.12	9.93	20.43	170.1	78
11	3.12	11.62	20.24	170.0	68
12	3.12	13.24	20.11	170.0	76
13	3.12	14.90	19.92	169.9	70
14	3.12	16.55	19.87	170.0	70
15	3.12	18.21	19.88	170.0	70

We propose a novel interpretation of the complexation mechanism between cadmium and penicillamine that involves protonated polynuclear complexes. This ineluctable conclusion is based upon evidence drawn from extensive potentiometric titrations specially designed to incorporate a new composition-of-species method.[14] The new method is an extension of the so-called FICS ("free ion concentration in solution"[15]) analysis developed by Osterberg,[16] Sarkar and Kruck,[17] McBryde,[18] and others.[15,19,20] The present study is the first experimental application of the new composition analysis to a system that contains polynuclear species.

Experimental Section

Chemicals. An acidified cadmium nitrate (J. Matthey, Puratronic grade) stock solution was prepared and analyzed by alkalimetric EDTA titrations and Gran plots.[21] D-penicillamine (Aldrich, Gold Label) was used to prepare a ligand stock solution, the concentration of which was determined by alkalimetric titrations. Potassium nitrate (J. T. Baker, *Analytical*) was used as a background electrolyte. All stock solutions were prepared and stored under moisture-saturated nitrogen in an inert atmosphere box.

Titration Method. Three groups of solutions were prepared in the inert box by dispensing aliquots of the stock solutions with a Gilmont precision glass-piston micrometer syringe. The 15 solutions (Table I) were initially acidified (HNO_3) and contained enough KNO_3 to produce a total ionic strength of 0.2 M. Each of the solutions in turn was titrated with standard KOH outside of the inert box, using the automatic titrator (vide infra). During the titrations, premoistened oxygen-free nitrogen was passed over the solutions. The temperature was maintained at 25 ± 0.1 °C.

Group I solutions (Table I, sets 1–3) contained penicillamine and were free of cadmium. Each of the group II solutions (sets 4–9) consisted of a different total cadmium concentration but the same total penicillamine concentration, with ligand-to-metal ratios, L/M (see Glossary of Terms), in the range 3–19. Conversely, each of the group III solutions (sets 10–15) contained a fixed amount of cadmium but a different amount of penicillamine, with L/M varying between 3 and 6. A total of 1061 pH measurements were collected in the pH range 1.9–12.5.

Electrode Calibration. A Beckman 39501 combination glass electrode was used. Before each titration, the pH meter settings were adjusted in the usual manner by using commercial pH 7 and 4 buffers. The pH meter readings were converted to those based on concentration with a universal buffer procedure.[23] Since the time between group titrations varied between 2 and 4 weeks, the electrode was recalibrated (to the concentration scale) for each of the three groups of titrations. (The titrations within a group were undertaken over a period of 1–2 days.) Equation 1 defines the conversion expression, where pH = −log [H^+], and

$$pH_{meter} = \Delta + S\,pH + j_H[H^+] + j_{OH}[OH^-] \quad (1)$$

typically $\Delta \sim 0.07$, $S \sim 1.007$, $j_H \sim 2.1$, and $j_{OH} \sim -1.5$.

Automatic Titrator. The computerized automatic titrator used in this study, an upgraded version of an earlier design,[23] consisted of a Cromemco Z80A 48K RAM microcomputer, a CP/M disk operating system with the Microsoft FORTRAN compiler, an Intertube II CRT terminal, an LA36 DECwriter, a HIPLOT digital plotter, and a Micromation dual-drive 8-in. floppy disk system. Interfaced to the computer were a Corning 130 pH meter, a magnetic stirrer, and a stepper-motor driven Gilmont precision glass-piston buret.

The automatic titrator utilized the FORTRAN program TITRATE[24] to collect and partially process the potentiometric data. Meter readings were deemed stable when the drift in pH was less than 0.005 pH min^{-1}.[23]

Method of Calculation. The extensive FORTRAN library of routines, STBLTY,[14,20,22,23,25] dealing with equilibrium analysis of potentiometric data, was used to reduce the data, develop the equilibrium model, refine the equilibrium constants, and perform an analysis of variance.

FICS (Free Ion Concentration in Solution) Analysis. Table II contains a glossary of terms used in the following descriptions. The concentrations of the free ion components in the mass balance equations (Table II) can be deduced from relations 2 and 3. The FICS procedure[14-20] first calls

$$pM = pM_0 - \int_{pH_0}^{pH} (\partial H/\partial M)_{pH,L}\, dpH|_M \quad (2)$$

$$pL = pL_0 - \int_{pH_0}^{pH} (\partial H/\partial L)_{pH,M}\, dpH|_L \quad (3)$$

for the construction of the constant-pH data $(H,M)_{pH,L}$ and $(H,L)_{pH,M}$ from the group II titration data, $(pH,H)_L$, and the group III titration data, $(pH,H)_M$, respectively. These transformations were effected by isohydric interpolation (using natural spline fitting[26]) of the two groups of titration curves. The discrete points in the transformed data were then fitted with deBoor's smoothing spline functions.[27] The first derivatives of the smooth functions were then used as integrands in eq 2 and 3. It is important that the above derivatives be evaluated at the total metal and ligand concentrations corresponding to the titration set that is common to both group II and group III series. This has been called the "common point",[20] and in the present case, sets 7 and 13 (Table I) are such points of intersection. At the intersection it is possible to deduce simultaneously the pM and pL values *without any assumptions as to the identities of actual complexes — mononuclear, polynuclear, or protonated polynuclear—which may be present in solution.*

ACSS (Average Composition of Species in Solution) Analysis. When the free concentrations of all of the reactants are known or can be calculated without knowledge of the nature of complexes present, as in the case of the "common point" data sets, it is possible to deduce the composition of species in solution. Under favorable experimental conditions, protonated polynuclear complexes can be identified. The required average stoichiometric coefficients, eq 4–6, may be calculated in the following manner (consult Table II for the glossary):

$$\bar{e}_m' = (M - m)/S' \quad (4)$$

$$\bar{e}_l' = (L' - l)/S' \quad (5)$$

$$\bar{e}_h' = (H' - h + K_w'/h)/S' \quad (6)$$

where

$$L' = L - l\sum_j^{N_h} h^j\beta_j^H \quad (7)$$

$$H' = H - l\sum jh^j\beta_j^H \quad (8)$$

$$S' = S - l\sum h^j\beta_j^H \quad (9)$$

$$S = \sum_j^N C_j \text{ (Sillén's "complexity sum")} \quad (10)$$

(13) Perrin, D. D.; Sayce, I. G. *J. Chem. Soc. A* **1968**, 53–57.
(14) Avdeef, A. *Inorg. Chem.* **1980**, *19*, 3081–3086.
(15) Guevremont, R.; Rabenstein, D. L. *Can. J. Chem.* **1977**, *55*, 4211–4221.
(16) Osterberg, R. *Acta Chem. Scand.* **1960**, *14*, 471–485.
(17) Sarkar, B.; Kruck, T. P. A. *Can. J. Chem.* **1973**, *51*, 3541–3548.
(18) McBryde, W. A. E. *Can. J. Chem.* **1973**, *51*, 3572–3576.
(19) Field, T. B.; McBryde, W. A. E. *Can. J. Chem.* **1978**, *56*, 1202–1211.
(20) Avdeef, A.; Raymond, K. N. *Inorg. Chem.* **1979**, *18*, 1605–1611.
(21) Gran, G. *Analyst (London)* **1952**, *77*, 661–671.
(22) Avdeef, A.; Sofen, S. R.; Brigante, T. L.; Raymond, K. N. *J. Am. Chem. Soc.* **1978**, *100*, 5362–5370.
(23) Avdeef, A.; Bucher, J. J. *Anal. Chem.* **1978**, *50*, 2137–2142.
(24) Avdeef, A., unpublished work.
(25) Avdeef, A. In "Computational Methods for the Determination of Stability Constants"; Leggett, D. J., Ed.; Plenum Press: New York, in press.
(26) Burden, R. L.; Faires, J. D.; Reynolds, A. C. "Numerical Analysis"; Prindle, Weber and Schmidt: Boston, 1978; pp 116–130.
(27) deBoor, C. "A Practical Guide to Splines"; Springer-Verlag: New York, 1978; Chapter 14.

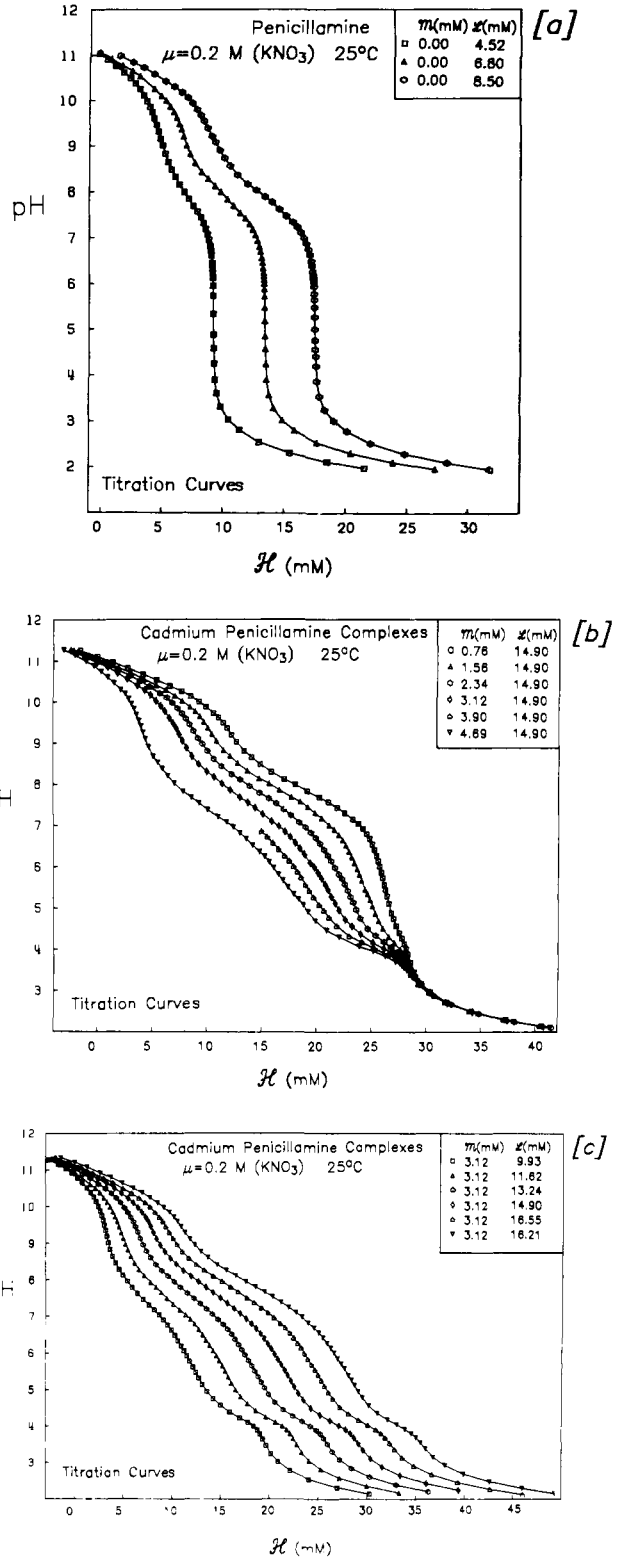

Figure 1. Titration curves, $(pH,H)_{M,L}$: (a) penicillamine in the absence of metal ions; (b) cadmium–penicillamine series with total metal concentration varied; (c) cadmium–penicillamine series with total ligand concentration varied.

The coefficient $\bar{e}_m'$ refers to the number of metal atoms in a complex at a particular pH. If more than one complex is present, then the coefficient refers to the number (not necessarily integral) of metal atoms averaged over all complexes. The $\bar{e}_l'$ and $\bar{e}_h'$ coefficients similarly refer to the number of ligand species and protons in the *metal-containing* complex(es). The Sillén sum, S (which is the crux of the ACSS analysis), was calculated by an integration method.[14]

Least-Squares Refinement of the Equilibrium Model. During the development of the equilibrium model, constants (in logarithmic form) were refined by a Gauss–Newton nonlinear weighted least-squares procedure. The function minimized was

$$S = \sum^{N_0}[(pM^{FICS} - pM^{calcd})^2/\sigma^2(pM) + (pL^{FICS} - pL^{calcd})^2/\sigma^2(pL) + (pH^{obsd} - pH^{calcd})^2/\sigma^2(pH)] \quad (11)$$

where the summation is carried over the number of pH measurements in the two "common point" sets (N_0 = 88 for pH 3.3–10.0). Superscript calcd. refers to the variable calculated as a function of a particular equilibrium model; superscript FICS refers to pM and pL determined by the FICS model independent method. The weighting scheme[22] was constructed from the variances:

$$\sigma^2(pX) = \sigma_c^2 + (\sigma_v\, dpX/dV)^2 \quad (12)$$

For pX = pM or pL, σ_c = 0.05; for pX = pH, σ_c = 0.02. In all cases σ_v = 0.001 mL. The term dpX/dV refers to the slope of the titration curve. One may note that the function minimized in our study is strategically different from those of other well-known programs, such as SCOGS[28] or MINIQUAD.[29] The goodness-of-fit, GOF, was defined as

$$GOF = [S/(3N_0 - N)]^{1/2} \quad (13)$$

where N refers to the number of constants.

As a final test of the validity of the model developed using only the "common point" sets of data, refinement with all 12 metal-containing titration data sets in the pH range 3.3–10.0 (N_0' = 553) was performed. The minimized function and the corresponding goodness-of-fit were defined as follows:

$$S' = \sum^{N_0'}(pH^{obsd} - pH^{calcd})^2/\sigma^2(pH) \quad (14)$$

$$GOF' = [S'/(N_0' - N)]^{1/2} \quad (15)$$

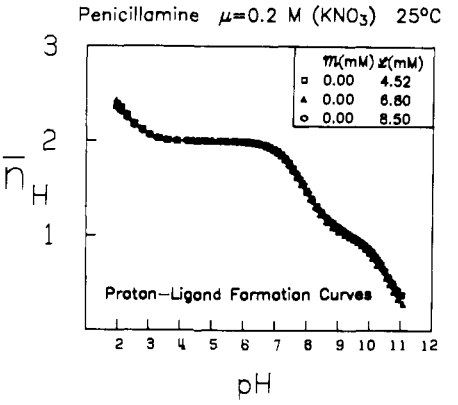

Figure 2. Formation curves for the penicillamine protonation reactions.

Results and Discussion

Ligand (Group I) Data. The titration curves for the three solutions containing penicillamine with no cadmium are shown in Figure 1a. The corresponding proton–ligand formation curves[30] ($\bar{n}_h$, pH) are depicted in Figure 2. The formation function $\bar{n}_h$ refers to the average number of bound protons per ligand in the absence of metal ions. Estimates of the protonation constants were obtained from the formation curves by using the half-$\bar{n}$ method.[31] These estimates were subsequently refined by least squares.

Metal Variation (Group II) Data. The six titration curves for the Group II solutions are shown in Figure 1b. The corresponding formation curves[30] ($\bar{n}$, pL), displayed in Figure 3a, reveal distinct dependence on the total cadmium concentration. This indicates that polynuclear and/or protonated metal–ligand complexes are present. (Only in the absence of protonated metal–ligand complexes does $\bar{n}$ refer to the average number of bound ligands per metal ion.) A most unusual feature in the formation curves is the apparent point at which all of the curves intersect, at $\bar{n}$ = 1

(28) Sayce, I. G. *Talanta* **1968**, *15*, 1397–1411.
(29) Sabatini, A.; Vacca, A.; Gans, P. *Talanta* **1974**, *21*, 53–77.
(30) Irving, H. M.; Rossotti, H. S. *J. Chem. Soc.* **1954**, 2904–2918.
(31) Rossotti, F. J. C.; Rossotti, H. "The Determination of Stability Constants"; McGraw-Hill: New York, 1961; pp 107–108.

Table II. Glossary of Terms

C_j	concentration of the jth associated species: $C_j = [M_{e_{mj}}L_{e_{lj}}H_{e_{hj}}] = \beta_j m^{e_{mj}} l^{e_{lj}} h^{e_{hj}}$
e_{kj}	stoichiometric coefficient, referring to the number of kth type of atoms in the jth associated species. For example, for the jth species $Cd(pen)_2(OH)$, $e_{mj} = 1$, $e_{lj} = 2$, $e_{hj} = -1$. The value of e_{hj} is negative to signify a hydroxide. Positive values refer to hydrogen atoms.
$\bar{e}_k$	average stoichiometric coefficient associated with the kth reactant at a particular pH
$\bar{e}_{k'}$	average stoichiometric coefficient of the kth reactant in *metal-containing* species
H	total hydrogen excess, defined as $A - B + 2L$, where $A = [HNO_3]$, $B = [KOH]$. The factor in front of L refers to the two dissociable protons introduced by the ligand. $H^{calcd} = h - K_w'/h + \Sigma_j^N e_{hj} C_j$
h	free hydrogen in concentration, $[H^+]$
oh	free hydroxide in concentration, $[OH^-]$
K_w'	$[H^+][OH^-]$, 1.78×10^{-14} at 25 °C and 0.2 M ionic strength
L	total concentration of the ligand: $L^{calcd} = l + \Sigma_j^N e_{lj} C_j$
l	concentration of the unassociated (and deprotonated) ligand
M	total concentration of the metal: $M^{calcd} = m + \Sigma_j^N e_{mj} C_j$
m	concentration of the free metal
$\bar{n}$	$= [L - (H - (h - oh))/\bar{n}_h]/M$
$\bar{n}_h$	$= \Sigma_j^N h_j h^j \beta_j^H / \Sigma h^j \beta_j^H$ for sets 4-15 (Table I) $= (H - (h - oh))/L$ for sets 1-3 (Table I)
N	number of associated species under consideration
N_h	maximum number of dissociable hydrogens on the ligand
pH, pL, pM	negative of the logarithm, base 10, of the corresponding free concentrations
pL_0 pM_0	integration constants
β_j	cummulative formation constant of the jth associated species, referring to the equilibrium expression $e_{mj}M + e_{lj}L + e_{hj}H \rightleftarrows M_{e_{mj}}L_{e_{lj}}H_{e_{hj}}$
β_j^H	protonation constant associated with the reaction $L + jH \rightleftarrows H_jL$

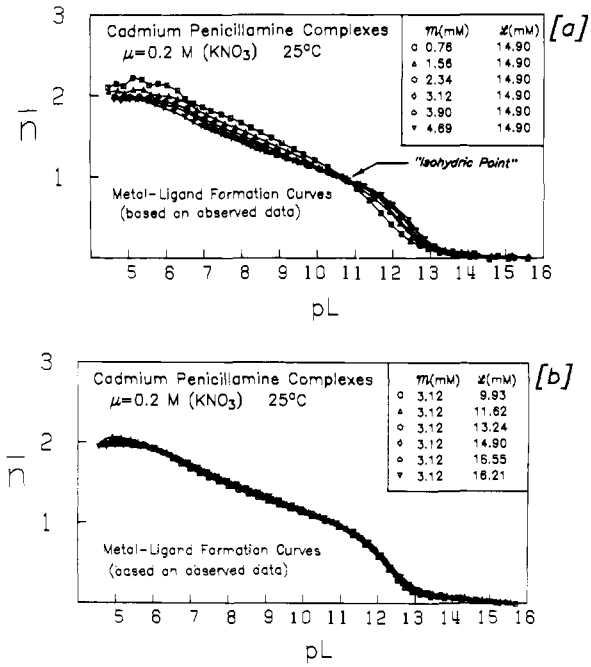

Figure 3. Metal–ligand formation curves calculated from observed data: (a) metal variation series; (b) ligand variation series.

and pL = 10.9 (pH 5.0). Such a point has been called an "isohydric point"[32-35] and has been likened to the isosbestic point found in absorption spectra. The half-$\bar{n}$ method is not valid for the estimation of equilibrium constants when formation curves display total concentration dependence.

Ligand Variation (Group III) Data. The titration curves for the group III solutions are shown in Figure 1c. The pertinent formation curves are displayed in Figure 3b. Within experimental uncertainty, the six formation curves show no dependence on the total penicillamine concentration.

FICS Treatment. Figure 4 shows the constant-pH curves $(H,M)_{pH,L}$ and $(H,L)_{pH,M}$, which are transformations of the primary potentiometric data from the groups II and III titrations. The plot of the partial derivative functions of the transformed data is shown in Figure 5. Integration of the latter curves as a function of pH leads to the determination of the pM and pL values, according to eq 2 and 3.

Deduction of the Equilibrium Model from the Functional Behavior of Data. The ACSS composition analysis (see Figure 6) narrowed the number of possible choices of complexes to rationalize the total metal concentration dependence of the formation curves in Figure 3a. Figure 6 in the pH 3–4 region suggests the metal-containing complex (if only one is present) has the composition $Cd(pen)H^+$. Such a species has already been reported.[9] The composition analysis further indicates the possible presence of protonated dimeric and trimeric metal complexes. The degree of condensation seems to maximize in the pH 5–6 region, the same region where the formation curves in Figure 3a appear to intersect. This latter relationship is theoretically expected.[33,34] For pH >8 mononuclear complexes once again predominate. They are not protonated since $\bar{e}_h'$ approaches zero.

Guided by the general trends in Figure 6, we began to test several combinations of species in order to simulate the observed functional form displayed in Figure 3a. We followed the bootstrap procedure suggested by Sillén (method of "species competition"[36]) with the aim of developing an equilibrium model having a minimum number of species and being consistent with the observed functional behavior of the data.

A satisfactory model was obtained which consisted of the species MLH, $M_3L_4H_2$, $M_3L_6H_4$, $M_2L_5H_3$, ML_2, and $ML_2(OH)$. Refinement of the model, using the two "common point" data sets, converged at the goodness-of-fit, GOF, value of 2.38. Refinement of the model proposed by Corrie et al.,[9] using our data, converged at the significantly higher value GOF = 3.25. In our model, the region of poorest fit was in the interval pH 6–7.5, where the species $M_2L_5H_3$ was postulated to predominate. We attempted to improve the fit by testing additional species that may have been important in that region, namely the species ML_2H, ML_3H_2, ML_3H, $M_4L_{10}H_6$, $M_4L_{10}H_4$, $M_6L_{15}H_9$, $M_8L_{10}H_{12}$. In all cases the GOF increased to 2.5–2.7. Thus none of these tested species was permanently accepted. In lower pH regions we included and ultimately rejected during refinement the following species: ML, ML_2H_2, M_3L_4H, $M_3L_6H_5$, $M_2L_5H_2$, and $M_2L_4H_4$. All of the latter species appeared reasonably consistent with the ACSS composition analysis. The addition of the hydrolysis species MOH, M_2OH, $M_4(OH)_4$ to the model did not affect the GOF. The calculated concentrations of the above species were extremely small.

(32) Carpeni, M. G. *Bull. Soc. Chim. Fr.* **1948**, 629–637.
(33) Bye, J. *Bull. Soc. Chim. Fr.* **1953**, 390–394.
(34) Souchay, P. *Bull. Soc. Chim. Fr.* **1953**, 395–399.
(35) Ingri, N.; Lagerström, M.; Sillén, L. G. *Acta Chim. Scand* **1957**, *11*, 1034–1058.
(36) Sillén, L. G. *Pure Appl. Chem.* **1968**, *17*, 55–78.

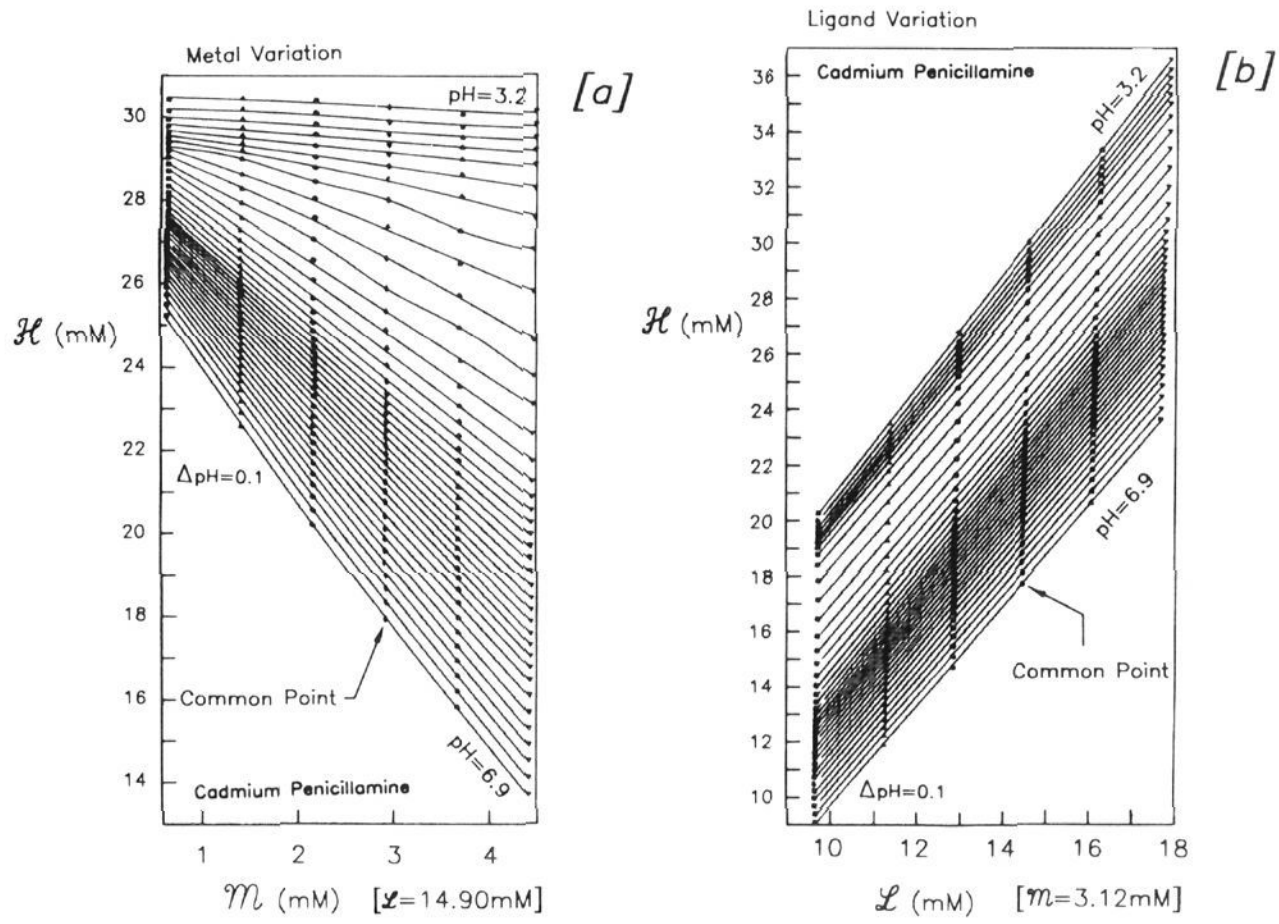

Figure 4. Transformed primary data for FICS analysis: (a) $(H,M)_{pH,L}$ data; (b) $(H,L)_{pH,M}$ data.

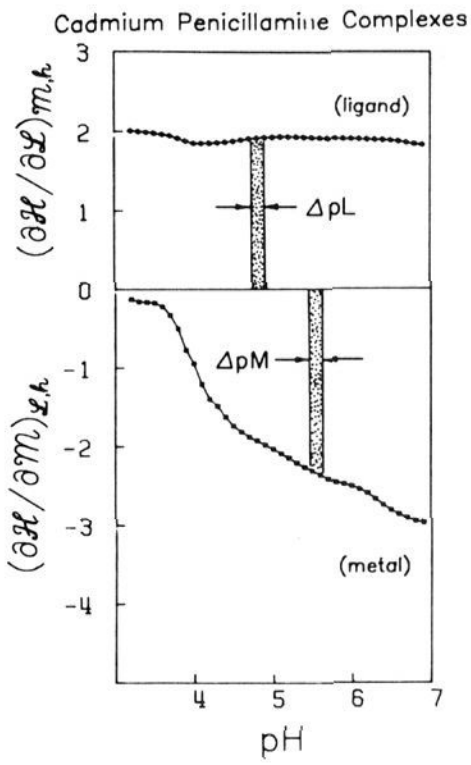

Figure 5. Integrand functions $(\partial H/\partial M)_{L,h}$ and $(\partial H/\partial L)_{M,h}$ for the determination of pM and pL values by the FICS method.

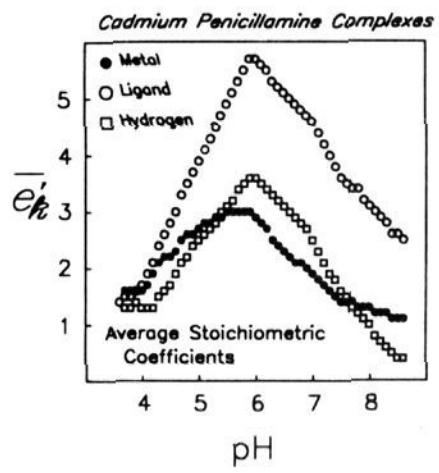

Figure 6. Average number of metal ($\bar{e}_m'$), ligand ($\bar{e}_l'$) and hydrogen ($\bar{e}_h'$) components in the metal-containing complexes (as determined by the ACSS method) as a function of pH.

"Core + Link" Component. In the final stages of model evolution it was noticed that the curves in the pH 6–7 region in Figure 6 appeared linear and might suggest a "core + link" family of complexes. Following the procedure developed by Sillén,[37,38] a plot of $\bar{e}_m'$ vs. $\bar{e}_l'$ in the pH 6–7 region produced the linear fit $\bar{e}_m' = 2.8 + 1.0\,\bar{e}_l'$. A plot of $\bar{e}_m'$ vs. $\bar{e}_h'$ produced the linear fit $\bar{e}_m' = 1.3 + 1.2\,\bar{e}_h'$. Rounding the coefficients to the nearest integral values yielded the "core + link" species $L_3H(MLH)_n$, which may be restated as $M_2L_5H_3(MLH)_n$ ($n = 0, 1, \ldots$). The species $M_2L_5H_3$ and $M_3L_6H_4$, already a part of the preceeding model, are the first two members of the series. The additional "core + link" components $M_4L_7H_5$ ($n = 2$) and $M_5L_8H_6$ ($n = 3$) were successfully incorporated into the model. However, higher order complexes in the series were not stable to refinement since their predicted concentrations were very small. On the basis of the refined values of the "core + link" constants (Table III), the series best fits Sillén's hypothesis IIIb: the first link forms more readily than the successive links, which form with nearly equal ease. (The number of species in the series is small, and it is not possible to rule out the IIIc hypothesis: formation of higher order species becomes increasingly more difficult.) The tetra- and quintanuclear

Table III. Refined Equilibrium Constants

ligand constants	this work		lit.[a]
pK_{a_1}	1.81 (3)[b]		1.90
pK_{a_2}	7.96 (1)		7.93
pK_{a_3}	10.72 (1)		10.66
metal–ligand log β constants	**"common point" data**	**all data**	**lit.[c]**
$Cd(pen)H^+$	16.66 (4)	16.39 (2)	17.15 (8)
$Cd_3(pen)_4H_2$	63.26 (8)	62.74 (12)	
$Cd_5(pen)_8H_6$[d]	134 (1)	133.8 (3)	
$Cd_4(pen)_7H_5^-$[d]	114.1 (3)	113.4 (2)	
$Cd_3(pen)_6H_4^{2-}$[d]	94.0 (1)	93.54 (4)	
$Cd_2(pen)_5H_3^{3-}$[d]	71.20 (8)	71.04 (4)	
$Cd(pen)_2^{2-}$	20.33 (2)	20.27 (2)	20.68 (6)
$Cd(pen)_2OH^{3-}$	9.87 (8)	9.74 (4)	9.14 (4)

[a] Ritsma, J. H.; Jellinek, F. *Recl. Trav. Chim. Pays-Bas* **1972**, *91*, 923. [b] The number in parentheses refers to the estimated standard deviation in the least significant digit of the corresponding constant. [c] Reference 9. [d] "Core + link" species, $M_2L_5H_3(MLH)_n$, $n = 0, 1, 2, 3$.

(37) Sillén, L. G. *Acta Chem. Scand.* **1954**, *8*, 299–317.
(38) Sillén, L. G. *Acta Chem. Scand.* **1954**, *8*, 318–335.

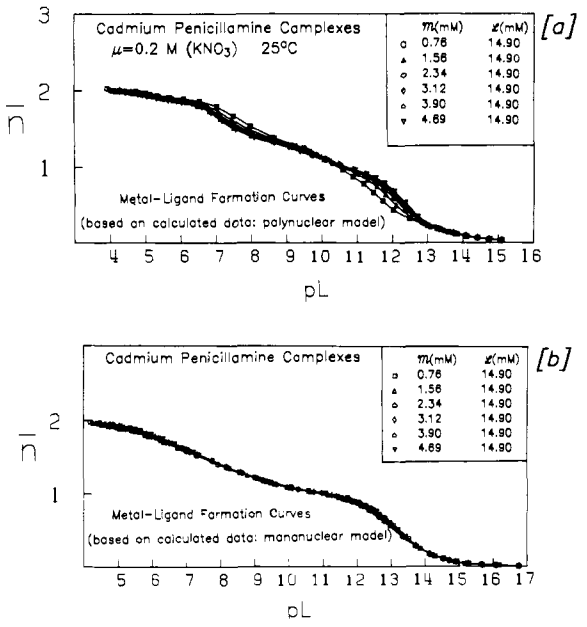

Figure 7. Metal–ligand formation curves calculated from *simulated* data: (a) simulated data using the final equilibrium model (Table III); (b) simulated data using the model proposed in ref 9.

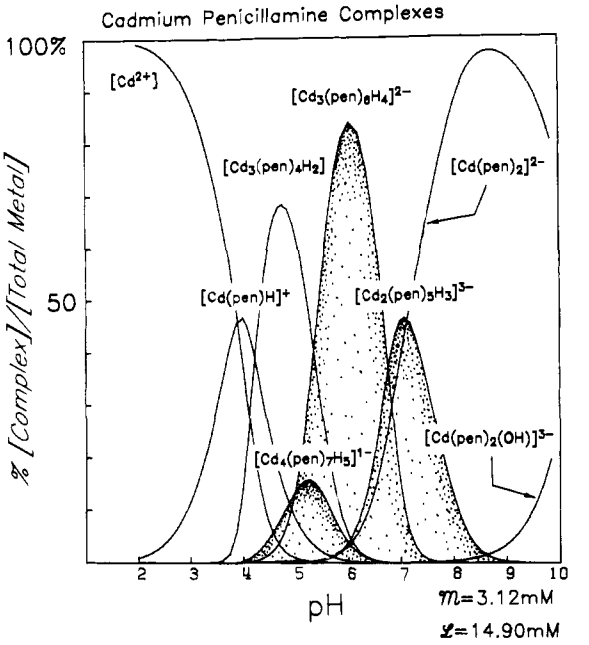

Figure 8. Distribution of species as a function of pH. Curves with shading identify the "core + link" species, n = 0, 1, 2.

species must be viewed as *only tentatively* identified, however, since their inclusion in the model did not effect significant changes in the GOF.

Calculated Formation Curves. The equilibrium model (including the "core + link" species up to n = 3) properly predicts a point of intersection ("isohydric point") in the metal-varied formation curves, as shown in Figure 7a (cf. Figure 3a). The metal concentration dependences are well simulated in the low pH region (pL 10–14 in Figure 7a). The simulation is less satisfactory in the higher pH region (pL 6–10).

The mononuclear model proposed by Corrie et al.[9] does not reproduce the functional behavior of the formation curves, as can be seen in Figure 7b.

Refined Constants. Table III summarizes the results of the refinement of the proposed equilibrium model. The pH-based refinement (eq 14) of constants where all 12 metal–ligand titration sets were used converged at GOF′ = 2.6. The constants refined

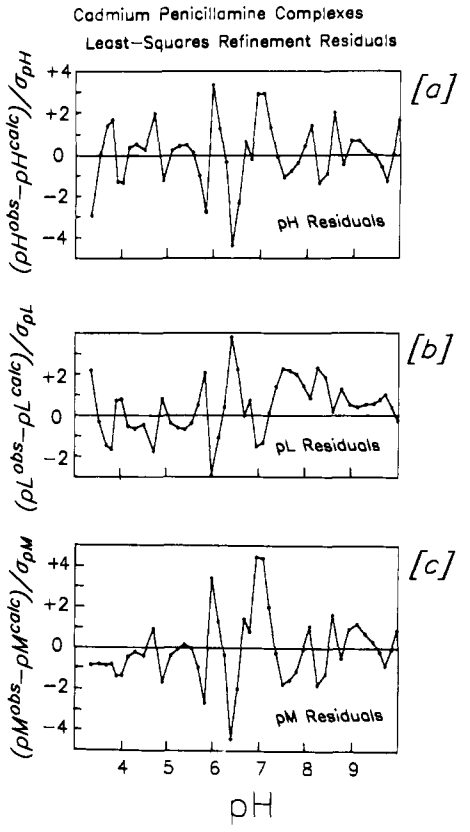

Figure 9. Weighted residual from least-squares refinement (see text).

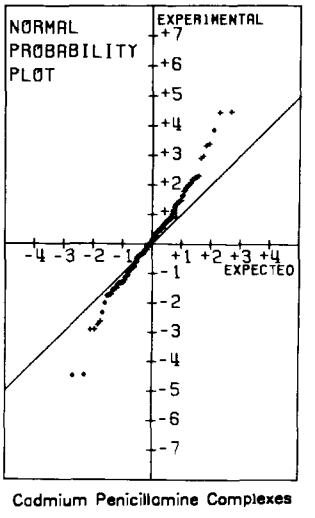

Figure 10. Abrahams–Keve normal probability plot (see text).

in such a manner are only slightly different from those based on the refinement using only the "common point" sets. Most of the differences are ≤3 units of standard deviation.

Description of Equilibrium Model. Figure 8 shows the distribution of species as a function of pH, at the total concentration of the "common point" sets. All of the polynuclear species are confined to the pH region 4–8. The "core + link" species (shaded areas under curves) predominate at pH 6. The pH 5 region, where the formation curves intersect in Figure 3a, principally contains the two species $Cd_3(pen)_4H_2$ and $Cd_3(pen)_6H_4^{2-}$. All of the polynuclear species are protonated and mostly anionic. In the basic pH region, mononuclear species $Cd(pen)_2^{2-}$ and $Cd(pen)_2(OH)^{3-}$ predominate.

Analysis of Variance. The least-squares residuals, based on pM, pL, and pH minimization (eq 11), are depicted in Figure 9. The weighted differences are uniformly distributed, with the larger

values occurring in the pH 6–7 region. Figure 10 shows an Abrahams–Keve[39] normal probability plot of the ordered weighted differences as a function of residuals expected from a Gaussian distribution of random errors of the same sample size. Although the observed distribution of errors is symmetrical about the zero value, the slope of the curve is larger than the expected value of unity. This can be interpreted to mean that either (a) unaccounted systematic errors are present and/or (b) our assigned weighting scheme slightly underestimates the true random errors in our observed data. Our inclination at present is to place more importance on the former interpretation, based on our favorable past experience with the weighting scheme used. Minor errors in the total concentration values can give rise to systematic effects of the magnitude observed.[40,41] An improper equilibrium model can also give rise to systematic errors. Of the large number of species tested, our present model appears to be the most satisfactory choice.

Conclusion

The functional form of the data in the present study persuasively argues for the case of polynuclear complexes. The composition analysis was crucial to our recognizing their presence. Evidence for such complexes may not have been apparent in the older studies of the cadmium–penicillamine system due to several possible factors: (a) total metal concentrations may not have been varied over a sufficiently broad range (or not varied at all); (b) data may not have been of sufficiently good quality to reveal the functional form; (c) the total metal concentrations may have been too low (<1 mM) to reveal polynuclear complexes. The study by Corrie et al.[9] was performed at 3 M ionic strength, so direct comparison of their findings to ours is probably not valid. The 3 M Na^+ concentration in the latter study may have caused unusual ion-pair reactions with the *anionic* clusters, perhaps suppressing their predominance.

Precedence for the trinuclear metal complex $Cd_3(pen)_4H_2$ may be found in the cysteamine–metal complexes studied by Jicha and Busch,[42] who proposed structure II. The IR study of solid-state

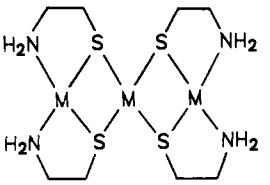

II

cysteine complexes of cadmium by Shindo and Brown[43] suggested the presence of the species $[M_3L_4^{2+}][MCl_4^{2-}]$. Their spectral evidence suggested that the amines were protonated and not bound to the metal atoms. They proposed structure III, in which the oxygen and sulfur atoms of cysteine are involved in the chelation.

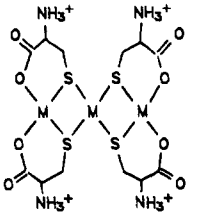

III

Coordination by the oxygen and sulfur atoms of penicillamine has been observed in the crystal structures of Cd(pen)[11] and Cd(pen H)Br.[12] The structure of the complex $Cd_3(pen)_4H_2$ proposed in our study may be similar to that of III, with the exception that only two groups (presumably amino) are protonated. If deprotonated amines are coordinated to the metal, as in II, then conceivably the structure of $Cd_3(pen)_4H_2$ may be depicted by IV.

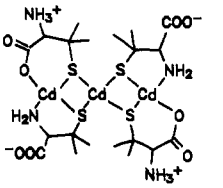

IV

Since potentiometric titration studies directly suggest composition and not structure of complexes, the verification of IV must await further studies by other techniques, such as ^{113}Cd NMR or X-ray crystallography.

Acknowledgment. Acknowledgment is made to the donors of the Petroleum Research Fund, administered by the American Chemical Society, for the partial support of this research. This project was also supported in part by BRSG Grant S07 RR07068-14, awarded by the Biomedical Research Support Grant Program, Division of Research Resources, National Institutes of Health, and the Research and Equipment Fund of Syracuse University, for which we are grateful. Technical assistance by William R. Eastwood and Larry D. Martin is gratefully acknowledged.

(39) Abrahams, S. C.; Keve, E. T. *Acta Crystallogr., Sect A.* **1971**, *A27*, 157–165.
(40) Sillén, L. G. *Acta Chem. Scand.* **1964**, *18*, 1085–1098.
(41) Anderegg, G. *Acta Chem. Scand.* **1980**, *A34*, 467.
(42) Jicha, D. C.; Busch, D. H. *Inorg. Chem.* 1962, *1*, 872–880.
(43) Shindo, H.; Brown, T. L. *J. Am. Chem. Soc.* **1965**, *87*, 1904–1909.